"Metabolic vulnerabilities and ferroptosis susceptibility in ARID1A-deficient endometrial carcinoma: Insights from metabolomics analyses"

Manel Albertí-Valls, Sara Olave, Xavier Matias-Guiu, Núria Eritja

Oncologic Pathology Group - Institut de Recerca Biomèdica de Lleida-IRBLleida. Universitat de Lleida, Hospital Universitari Arnau de Vilanova (HUAV), Lleida, Spain. Centro de Investigación Biomédica en Red en Cancer (CIBEROnc)

Introduction & Objectives

ARID1A is a gene encoding for ARID1A, a member of the ATP-dependent chromatin remodeling complex SWI/SNF. Previous findings have shown that ARID1A acts as a driver gene in the development of the metastatic phenotype. Our group has already described that the loss of ARID1A expression in endometrial cancer (EC) induces more aggressive tumor phenotypes promoting the transition to a mesenchymal phenotype (EMT) and acquiring greater migratory and invasive capacities bypassing G2/M cell cycle checkpoints. In this study, we used three sets of paired EC cell lines: those with ARID1A depletion and their wild-type counterparts, as well as 21 patient tumor samples with ARID1A deficiency and 19 with ARID1A wild-type expression, and applied large-scale metabolomics and a variety of functional analyses to draw a precise picture of the metabolic landscape of ARID1A-deficient EC and undercover novel pharmacological vulnerabilities based upon this information.

1. Metabolomics assay reveals a unique metabolic profile in ARID1A-deficient EC.

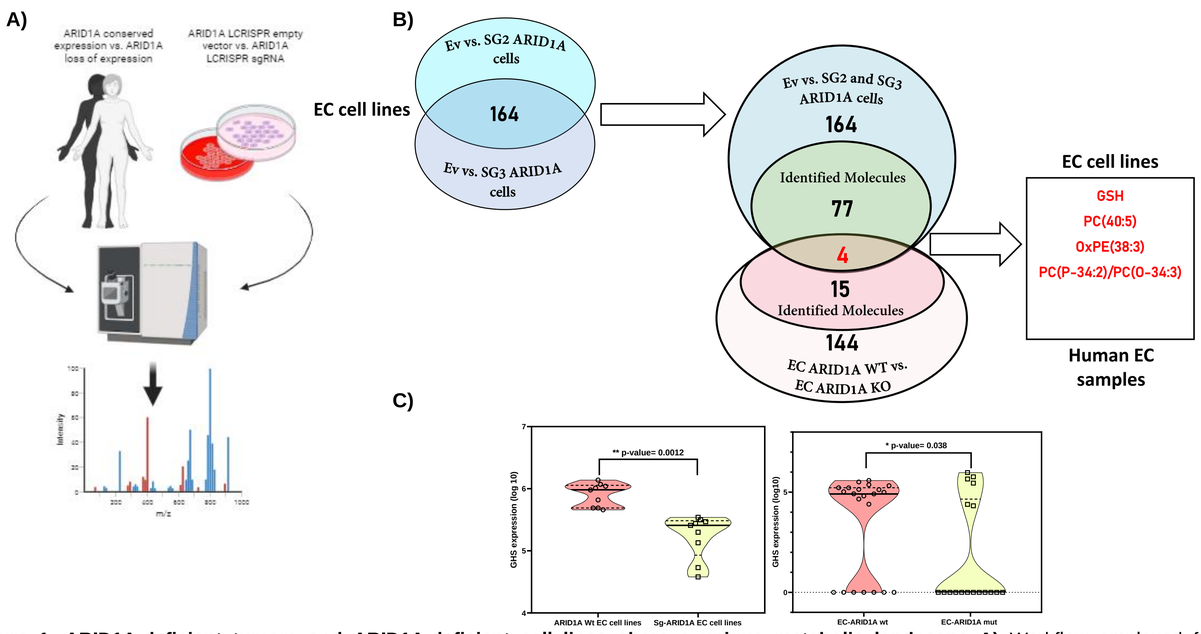

Figure 1. ARID1A-deficient tumors and ARID1A-deficient cell lines share a unique metabolic landscape A) Workflow employed for metabolomics. Three paired EC cell lines infected with two different sgRNA-ARID1A (SG2 and SG3) plasmids and Human tumor samples with wild-type and aberrant ARID1A expression were studied. Samples were processed via LC-MS/MS and untargeted metabolomics analysis were applied. **B)** Venn diagram. An ANOVA analysis was performed, grouping samples by cell line type and different between sgRNA-ARID1A interferences, a total of 206 differential metabolites emerged with a p-value corrected for FDR < 0.05. Of these, 156 were differential in both SG3 and SG2 conditions and had the same behavior in both. Finally, 77 of these were identifiable and four were shared between EC cell lines and human tumor samples. Reduced Glutathione (GSH), as well as Phosphocoline (PC) 40:5 and other species prone to peroxidation were detected as the common differential metabolites. C) Data from GSH levels is shown.

2. ARID1A-deficient EC cells have alterations in lipid metabolism.

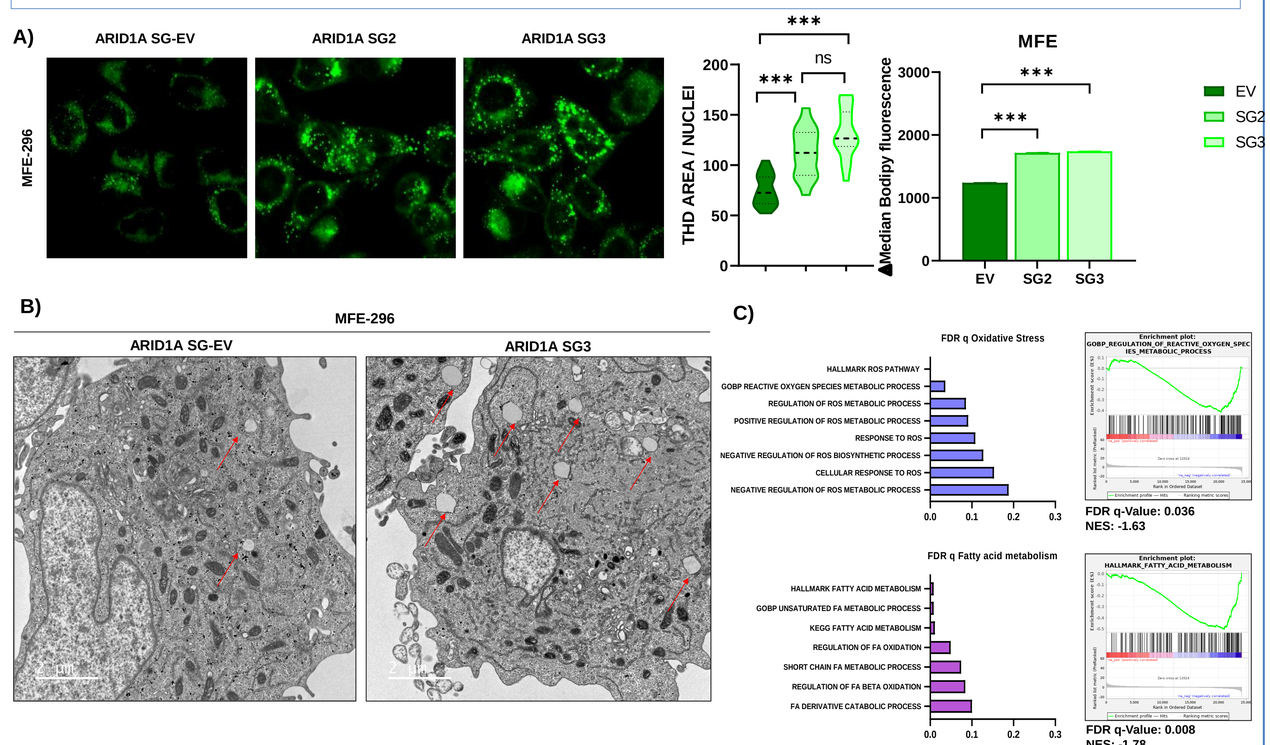

Figure 2. Lipid metabolism and ROS homeostasis pathways are altered in ARID1A-deficient EC Cell lines. A) Bodipy 493/503 ICC reveals an increased accumulation of Neutral Lipid Droplets in ARID1A-depleted EC Cell Lines. Left: representative images; Middle: Data expressed as fluorescence level of thresholded area divided by number of cells; Right:: FACS analysis of the same samples showed that ARID1A-depleted EC Cell Lines accumulate LDs, as well. (ANOVA analysis was performed ***p<0,001) **B)** Transmission electronic microscopy reveals LD accumulation in MFE-296 ARID1A-depeleted cells, as well. Red arrows indicate LDs. Representative images are shown. **C)** Gene set enrichment analysis (GSEA) from multiple repositories (KEGG and GOBP) gives further insight on the relevance of ARID1A regulation in these pathways and supports our in vitro evidence.

3. ARID1A deficiency drives GPX4 expression across multiple EC models

Figure 3. ARID1A deficiency drives GPX4 expression across multiple models. A) Representative western blot (left) and qPCR (right) of MFE-296 samples. **B)** GPX4 expression data from the TCGA. Data is plotted as log2 of expression. **C)** Representative IHC images of ARID1A and GPX4 from TMA of 160 patient samples from HUAV. Image analysis was performed with QuPath: Middle graph shows share of staining levels. Right graph shows total gland histoscore. **D)** Representative IHC images of ARID1A and GPX4 transgenic mice strains with induceable knockout of PTEN and ARID1A. Graph below shows GPX4 gland histoscore. (ANOVA analysis was performed **p<0,001).

4. ARID1A depleted cell lines are more sensitive to ferroptosis induction than those with wild type ARID1A expression

Figure 4. GPX4 buffers PUFA and generates LDs to avoid ferroptosis in ARID1A depleted EC Cell Lines. A) Viability assays at different doses of RSL3 ± Ferrostatin-1. **B)** BODIPY C11 was used to assess basal and RSL3 levels of lipid peroxidation. Data is expressed as % of Max values **C)** Clear-field images of MFE 296 Cells (ARID1A wt expression and ARID1A KD expression) after RSL3 treatment. **D)** Western blot analysis of GPX4 levels upon RSL3 treatment (time –dependent inhibition) ± Ferrostatin-1. Representative images are shown.

Conclusions

The data presented shows that ARID1A is a relevant player in lipid metabolism and how its loss of expression in an oncogenic context can generate vulnerabilities to ferroptosis inductors such as RSL3.

Supported by grants from: Fundación Contigo (ENDARMA project), CIBERONC CB16/12/0023; ISCIII/FEDER 'Una manera de hacer Europa'' ''PI20/00502 and 2021 SGR00093.
MAV holds a predoctoral fellowship from Universitat de Lleida ''Ajuts predoctorals per a nous investigadors''.